Cell, Vol. 121, 375–385, May 6, 2005, Copyright ©2005 by Elsevier Inc. DOI 10.1016/j.cell.2005.03.011

Acetylation in Histone H3 Globular Domain Regulates Gene Expression in Yeast

Feng Xu,[1] Kangling Zhang,[2] and Michael Grunstein[1,*]
[1]Department of Biological Chemistry
Geffen School of Medicine at UCLA
and the Molecular Biology Institute
University of California, Los Angeles
Boyer Hall
Los Angeles, California 90095
[2]Mass Spectrometry Facility
Department of Chemistry
University of California, Riverside
Riverside, California 92521

Summary

In *Saccharomyces cerevisiae,* known histone acetylation sites regulating gene activity are located in the N-terminal tails protruding from the nucleosome core. We report lysine 56 in histone H3 as a novel acetylation site that is located in the globular domain, where it extends toward the DNA major groove at the entry-exit points of the DNA superhelix as it wraps around the nucleosome. We show that K56 acetylation is enriched preferentially at certain active genes, such as those coding for histones. *SPT10*, a putative acetyltransferase, is required for cell cycle-specific K56 acetylation at histone genes. This allows recruitment of the nucleosome remodeling factor Snf5 and subsequent transcription. These findings indicate that histone H3 K56 acetylation at the entry-exit gate enables recruitment of the SWI/SNF nucleosome remodeling complex and so regulates gene activity.

Introduction

Eukaryotic DNA is packaged in nucleosomal particles for assembly into higher-order structures in the nucleus. These particles contain four core histones (H2A, H2B, H3, and H4), which form a protein octamer that is wrapped by almost two turns or 146 bp of DNA. However, the nucleosomal core particle is a dynamic structure that can participate in gene regulation and higher-order folding through specialized histone domains. Each histone contains a charged N-terminal region adjacent to a globular structured domain containing α-helical histone folds. As observed in the nucleosome core particle high-resolution X-ray structure, the histone N-terminal tails extend from the core of the nucleosome and pass between the gyres of the DNA superhelix where they may interact with adjacent nucleosomes (Luger et al., 1997a). The N termini are also the targets of enzymes that add or remove acetyl, methyl, and phosphate groups that help modulate the function of the histone proteins. These posttranslational modifications and the N-terminal tails themselves have little effect on nucleosome stability (Luger et al., 1997a). However, the tails are required for higher orders of chromatin fiber folding in vitro that may affect access to transcription factors (Dorigo et al., 2003). In addition, the histone N termini serve as binding sites for transcriptional regulators. For example, in yeast, both repressor proteins, such as Sir3, and transcriptional activators, such as the bromodomain-containing protein Bdf1, interact with the histone H4 N terminus. These interactions are regulated by histone acetyltransferases (HATs) and deacetylases (HDACs) (Carmen et al., 2002; Hecht et al., 1995; Ladurner et al., 2003; Matangkasombut and Buratowski, 2003). In addition, repressor proteins such as HP1 and Polycomb in higher eukaryotes recognize the methylated H3 N termini (Bannister et al., 2001; Lachner et al., 2001). These data argue that the histone N termini and their modifications may regulate gene activity not through regulating nucleosome stability or nucleosomal conformation but in regulating higher-order structures and by the direct recruitment of regulatory proteins (for review see Workman and Kingston [1998]).

In the globular region of each histone, the central histone fold domains contain three α-helical regions separated by L1 and L2 loops (e.g., α1-L1-α2-L2- α3; Luger et al., 1997a). There are also helical extensions in H3 and H2B histones that are N- and C-terminal to the central histone folds, respectively. In contrast to the N termini, the histone-folds interact extensively with DNA. Of the 146 bp wrapped around the histone octamer in the X-ray crystal structure, 121 bp interact with the histone fold region. In addition, the α-helical histone-fold extension of H3 (H3 αN) selectively binds to the remaining 13 base pairs of DNA where the DNA superhelix enters and exits the nucleosome (Luger et al., 1997a; White et al., 2001). Thus, through their extensive interactions with DNA, the central histone folds and extensions, but not the histone tails, are important in stabilizing the nucleosome core particle (Luger et al., 1997b).

Regulators that do affect nucleosome stability include nucleosome remodeling complexes such as SWI/SNF. Remodeling complexes use the energy of ATP hydrolysis to alter nucleosome structure and translational position on DNA (Peterson and Workman, 2000; Workman and Kingston, 1998), in some cases by changing DNA conformation at the nucleosomal entry-exit sites (Langst and Becker, 2001). An electron microscopy study indicates a loss of DNA content from nucleosomes remodeled by SWI/SNF (Bazett-Jones et al., 1999), probably as a result of unwrapping of some 50 bp of DNA from the edges of the nucleosome (Kassabov et al., 2003; Lorch et al., 2001). This may result in the exposure of DNA on the nucleosomal surface (Becker and Horz, 2002), the sliding of nucleosomes to new positions (Meersseman et al., 1992), and the eventual loss of nucleosomes from highly active genes (Boeger et al., 2003; Narlikar et al., 2002; Reinke and Horz, 2003).

There is clearly interplay between nucleosome remodeling complexes and those mediating histone acetylation. Activators can recruit both types of complexes

*Correspondence: mg@mbi.ucla.edu

to promoters (Cosma et al., 1999; Kingston and Narlikar, 1999). However, the temporal order of these activities can vary. In vitro, histone N-terminal acetylation stabilizes the binding of the SWI/SNF complex to nucleosome arrays (Hassan et al., 2001). SWI/SNF action at certain yeast promoters recruits HAT activity (Cosma et al., 1999; Krebs et al., 1999), while acetylation is required for SWI/SNF function at certain mammalian promoters (Agalioti et al., 2000; Dilworth et al., 2000). In either case, it appears that acetylation of the histone tails does not strongly destabilize the nucleosome, but the action of SWI/SNF does.

For acetylation to directly affect histone-DNA interactions of the DNA superhelix surrounding the histone octamer, it could potentially occur in the histone globular domain. However, while more than 25 acetylation and methylation sites have been discovered in regions outside of the N termini of calf histones, their functions are still unknown (Zhang et al., 2003). A genetic analysis using yeast could uncover such functions; however, all of the known acetylation sites in core histones of *S. cerevisiae* are located in the N-terminal tails. We now describe a site of acetylation (histone H3 K56) found in the globular domain of a yeast histone. This novel acetylation site is located in the αN extension of the H3 histone fold. We demonstrate that disruption of the putative HAT *SPT10,* but not of six other HATs examined, strongly decreases the S phase-specific acetylation of this site at histone genes and prevents recruitment of Snf5, an essential member of the SWI/SNF nucleosome remodeling complex (Geng et al., 2001), and subsequent transcription. These data argue for the role of histone H3 K56 modification in regulating the entry-exit gate to nucleosome remodeling.

Results

Lysine 56 in the αN Histone Fold Extension of H3 Is Acetylated in *Saccharomyces cerevisiae*

To search for new modification sites, yeast core histones were purified from asynchronously growing cells and examined by mass spectrometry. We found that lysine 56 within the αN domain of histone H3 is acetylated (see Figure S1 in the Supplemental Data available with this article online) at ~28% of H3 molecules (data not shown). To further investigate the role of K56 acetylation in vivo, we first generated an antibody specific for this acetylation site using a synthetic K56 Ac peptide (Figure S2A; Experimental Procedures). Specificity of the anti-H3 K56 acetylation-site antibody (α-K56 Ac) was tested sequentially by ELISA, Western blot, and chromatin immunoprecipitation (ChIP) against histone mutations as described earlier (Suka et al., 2001; Turner and Fellows, 1989). In ELISA, only the peptide containing acetylated K56 strongly inhibits antibody binding to the K56 Ac-KLH conjugate coated to the microtiter plate (Figure S2B). In Western blots, α-K56 Ac strongly immunoreacts with histone H3 from wt strains, and those in which another H3 acetylation site has been mutated (H3 K14R) but showed no detectable reactivity toward H3 whose K56 residue had been mutated (K56G, K56R; Figure S2C). Finally, ChIP assays were performed using chromatin from wt and K56G mutant strains. As shown in Figure S2D, the K56G mutation strongly reduced the PCR amplification of the *HTA2* coding region (normally 5.8-fold over background) to background levels. Together, these data demonstrate that antibody α-K56 Ac is highly specific for acetylated K56 in histone H3.

Hyperacetylation of H3 K56 Is Associated with Histone Genes

The combination of ChIP and DNA microarrays has been widely used in genome-wide analyses to determine the locations of protein binding and histone modification (Kurdistani et al., 2002; Lieb et al., 2001; Ren et al., 2000; Robyr et al., 2002). To map H3 K56 acetylation throughout the genome, we isolated chromatin fragments immunoprecipitated (IP) with α-K56 Ac from formaldehyde-treated cells. Both the IP and input DNA were purified, amplified by PCR, and labeled with a fluorophore (Cy3 or Cy5). The labeled IP and input DNA were combined and hybridized to a DNA microarray containing ~6700 intergenic regions (IGRs; prepared in house) or >6200 open reading frames (ORFs; University Health Networks, Toronto). Both IGRs and ORFs microarray experiments were repeated three times from independently prepared ChIP DNA samples, and the K56 acetylation data of 5625 ORFs and 5606 IGRs were available for further analysis (Table S1).

We asked whether genes that are hyperacetylated at H3 K56 are significantly enriched in any of the known categories of biological function, fitness, protein complexes, etc. FunSpec (Functional Specifications at http://funspec.med.utoronto.ca), which contains a comprehensive database of these features, was used and identified all of the eight core histone genes to be among the top 123 hyperacetylated ORFs (>1.6-fold). Among the 123 genes, only the histone genes fell into a known functional category (the chromosome functional category, p = 1.72E-06) in the MIPS functional category database and the nucleosomal protein complex category (p = 1.79E-14) in the MIPS protein complex database.

To determine whether K56 acetylation correlates with that of other known histone acetylation sites, we compared our data to that of Kurdistani et al. (2004), who examined the genome-wide occurrence of acetylation at 11 sites of acetylation in all four core histones. We did not find there to be a strong correlation of K56 acetylation with any of other N-terminal sites of acetylation (data not shown). While many sites of histone H3 N-terminal acetylation showed correlations R > 0.8 in pairwise comparisons (Kurdistani et al., 2004), the maximal correlation between K56 acetylation and other sites was R = 0.30 with H3 K18 (ORFs) and R = 0.19 with H3 K9 (IGRs). These data may be explained if a subset of active genes throughout the genome is affected strongly by K56 acetylation and if K56 acetylation is due to a distinct HAT at these genes.

H3 K56 Acetylation Is Mediated by the Putative HAT Spt10 at Histone Genes

To search for the enzyme(s) responsible for K56 acetylation state, we used ChIP to examine the effects of mutations of the known HATs and HDACs at individual genes identified in the microarrays as being enriched

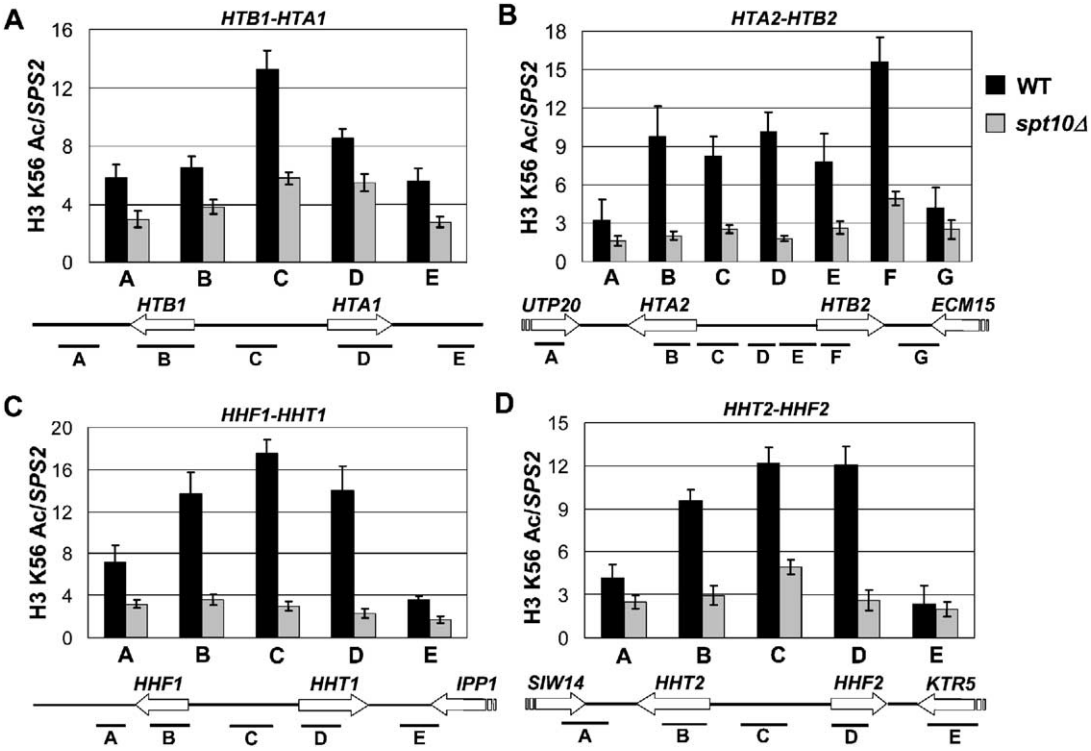

Figure 1. Effects of *spt10Δ* on H3 K56 Acetylation at Histone Genes

Relative H3 K56 acetylation and histone H3 levels were determined by ChIP assays using α-K56 Ac and α-H3-C antibodies and normalized to an internal control (*SPS2)* and the input DNA. The relative level of K56 acetylation was then normalized to that of histone H3. The K56 acetylation level decreases dramatically at (A) *HTB1-HTA1*, (B) *HTA2-HTB2*, (C) *HHF1-HHT1*, and (D) *HHT2-HHF2* genes upon *SPT10* deletion. *spt10Δ* affects K56 acetylation at both the promoter and coding region of all the histone genes. K56 acetylation at most adjacent regions around histone genes is affected to a lesser extent. The gene map under each graph shows the positions of fragments amplified in PCR. The results are averages of three independent ChIPs with error bars shown for standard deviations.

for K56 acetylation. Of the HAT (*ELP3*, *GCN5*, *SAS2*, *SAS3*, *ESA1*, *SPT10*, *NUT1*) and HDAC (*HDA1*, *HOS1*, *HOS2*, *HOS3*, *RPD3*) disruption strains examined for acetylation changes at both the promoter and coding regions of histone genes, only one, containing a disruption of the putative HAT *SPT10*, was shown to be required for acetylation of H3 K56 (Figure S3). To analyze the extent of K56 acetylation along the various histone promoters and coding regions and the involvement of *SPT10* in their acetylation, we examined both IGRs and coding regions at all histone genes. We corrected for nucleosome loss during gene activity (Boeger et al., 2003; Reinke and Horz, 2003) by determining the presence of histone H3 at histone genes using an antibody directed to the unmodified C terminus of H3 (Gunjan and Verreault, 2003). The acetylation data was then normalized to the level of histone H3 in both wt and mutant strains. We estimate that there is a 1.6- to 6.2-fold decreased K56 acetylation in the *spt10Δ* strain as compared to wt cells at all core histone genes (Figure 1). Therefore, given that Spt10 has previously been shown to bind to the promoters of histone genes (Hess et al., 2004) and is required for histone gene expression, Spt10 is likely to be directly required for acetylation of H3 K56 at histone genes.

In order to determine the extent to which Spt10 binds to histone gene ORFs as well as at promoters, we examined the binding of myc epitope-tagged Spt10 at the histone genes. We found that Spt10-myc binds stronger at promoters than coding regions at all histone genes with the most binding at the promoters of *HTA1* and *HTB1* genes (18 fold enrichment as normalized to negative control and input, Figure 2). Spt10-myc binds 2.2- to 2.6-fold better at coding regions of all histone genes than to adjacent nonhistone IGRs and ORFs. Therefore, while Spt10 is highly enriched at histone gene promoters, it also binds at a lower but significant level to adjacent histone ORFs.

We then wished to determine the sites of acetylation in all core histones affected by the loss of Spt10 at the histone genes. Using highly specific antibodies against 12 individual sites of acetylation in all core histones (Suka et al., 2001), we found that *spt10Δ* affects mainly H3 K9, K18, and K56 acetylation at the coding region of the *HTA2* gene with the greatest effect occurring on K56 acetylation (~5.2-fold; Figures 3A and S4). Similar findings were made at the intergenic region of *HTA2* (data not shown). We did not detect comparable differences in the extent of acetylation at the other histone H3 sites (Figure 3A) nor at sites in H4 (Figure S4A), H2A, and H2B (Figure S4B) histones. Therefore, Spt10 is specific for H3 K56, K18, and K9 at histone genes.

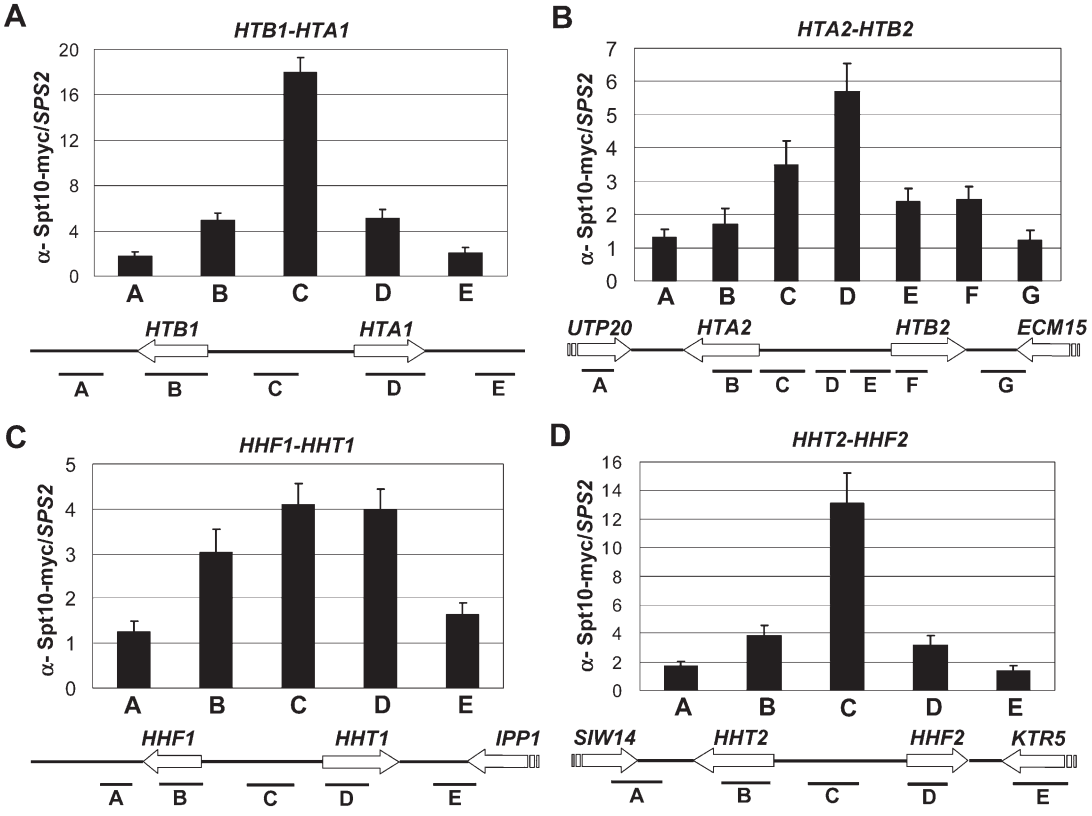

Figure 2. Spt10 Binds at All of the Histone Genes

Spt10 × 13myc binding assays were performed using an antibody against Myc tag. The binding data are normalized to an internal control (*SPS2)* and the input DNA. Spt10 binds at both the promoter and coding region of (A) *HTB1-HTA1*, (B) *HTA2-HTB2*, (C) *HHF1-HHT1*, and (D) *HHT2-HHF2* genes. Generally, Spt10 binds better at promoters than coding regions of histone genes but less so at adjacent regions around histone genes. The gene map under each graph shows the positions of fragments amplified in PCR. The results are averages of three independent ChIPs with error bars shown for standard deviations.

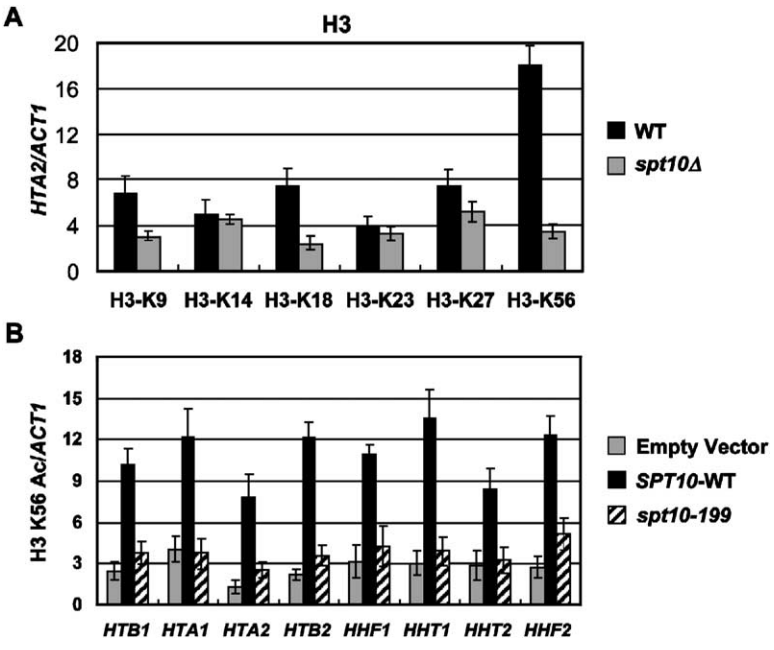

Figure 3. Role of *spt10Δ* and HAT Domain Mutation *spt10-199* on Specific Sites of Acetylation in Histone H3

(A) ChIPs using antibodies specific for individual acetylation sites on histone H3 tails. Acetylation sites examined are indicated below the graph. A primer pair targeting the *HTA2* coding region was used in PCR and normalized to the *ACT1* coding region. All of the acetylation data were normalized to the level of histone H3.

(B) H3 K56 acetylation levels at the coding region of all the core histone genes are reduced in Spt10 HAT domain mutant *spt10-199* to the similar level of an *spt10Δ* strain harboring an empty vector. Samples were taken at 50 min after *cdc15*^{ts} cells were released from the restrictive temperature (37°C) to permissive temperature (23°C). These results are averages of three independent ChIPs with error bars shown for standard deviations.

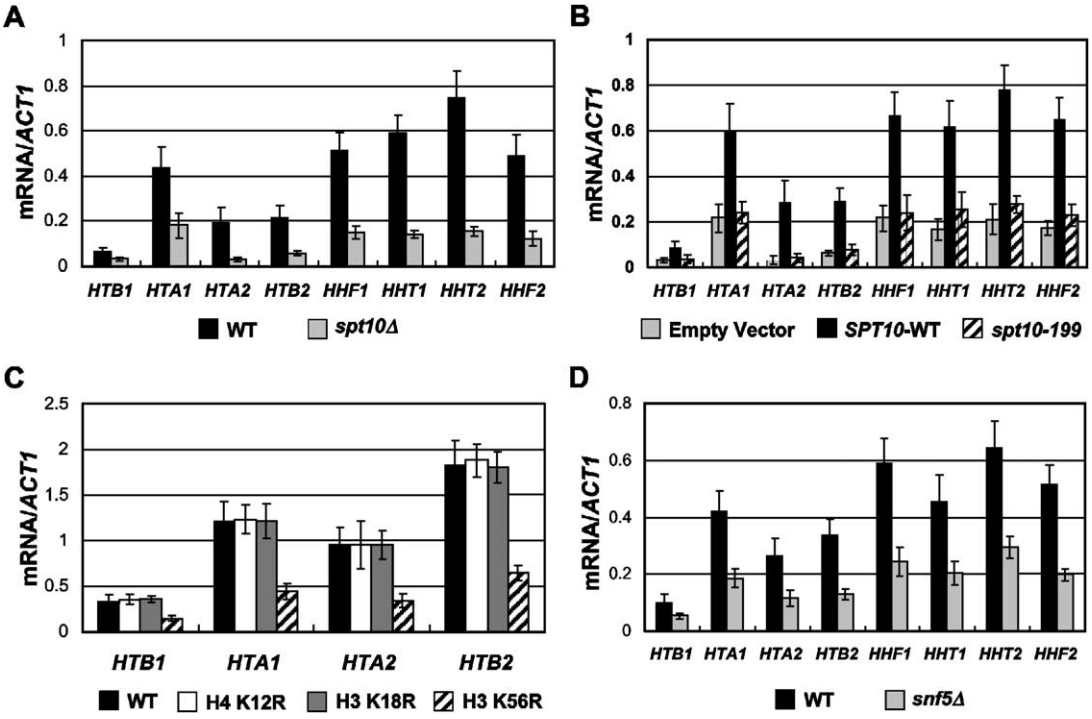

Figure 4. *spt10⊿*, *spt10-199*, H3 K56R, and *snf5⊿* All Affect Histone Gene Expression in a Similar Manner

Histone mRNA levels affected by (A) *spt10⊿*, (B) *spt10-199*, (C) H3 K56R, and (D) *snf5⊿* mutations. In (B), samples were taken at 75 min after *cdc15^{ts}* cells were released from the restrictive temperature (37°C) to permissive temperature (23°C). In (C), H4 K12R and H3 K18R mutations are used as controls and are shown not to affect histone gene expression. Histone mRNAs were amplified by quantitative RT-PCR and normalized to *ACT1* transcript. Values are averages of three independent experiments with error bars shown for standard deviations.

Spt10 shares a conserved acetyltransferase domain with other HATs, including Gcn5 (Neuwald and Landsman, 1997). A mutant allele *spt10-199* containing G199A and G201A changes within the HAT domain has virtually the same strong defect as an *spt10⊿* mutant in histone gene activation (Hess et al., 2004). Therefore, we asked whether *spt10-199* also affects K56 acetylation at histone genes. We found that K56 acetylation was reduced between 2.7-fold (*HHF2*) and 3.8-fold (*HHT1*) in the *spt10-199* mutant as compared to the wt strain (Figure 3B). The decrease of K56 acetylation in *spt10-199* is almost as severe as in the *spt10⊿* strain harboring an empty vector. These data indicate that the Spt10 acetyltransferase domain is essential for K56 acetylation at histone genes.

Spt10, K56 Acetylation, and Snf5 Are All Required for Histone Gene Expression

We then asked whether Spt10 regulates transcription of all histone genes. As previously reported, Spt10 is required for expression of a subset (*HTA2*, *HTB2*, *HHF2*, and modestly at *HHT2*) of histone genes (Hess et al., 2004). In this study, we show by quantitative RT-PCR that activity of all of the histone genes is dependent on *SPT10*. As compared to the wt strain, there is a decrease of between 6.7-fold (*HTA2*) and 2-fold (*HTB1*) in the histone mRNA levels in the *spt10⊿* strain (Figure 4A). Similar decreases in histone gene transcription are seen in the *spt10-199* allele (Figure 4B). Therefore, *SPT10* and its catalytic domain are required for all histone gene activity.

To determine whether the effect of *SPT10* on transcription is mediated through K56, we then examined the effect of K56R on the expression of genomic H2A and H2B genes. As shown in Figure 4C, H3 K56R results in a 2.3- to 2.9-fold decrease in the expression of all four H2A and H2B genes as compared to the wt strain or as compared to H3 K18R (another site affected by *spt10⊿*) and H4 K12R (that is not affected by *spt10⊿*). Therefore, K56 in histone H3 is uniquely important for transcription of the histone genes examined.

Previous studies demonstrated that an essential subunit of the SWI/SNF nucleosome remodeling complex, Snf5, is required for full expression of histone *HTA1-HTB1* genes (Dimova et al., 1999). Thus, we examined the effects of *snf5⊿* deletion on other histone genes in this study. As shown in Figure 4D, *snf5⊿* significantly reduces the expression of all the histone genes from 1.9-fold (*HTB1*) to 2.6-fold (*HTB2*). These data indicate that Spt10 through its catalytic domain, H3 K56, and the SWI/SNF remodeling complex affect expression similarly at all histone genes examined.

H3 K56 Acetylation at Histone Genes (*HTA1*, *HTA2*) Is Uniquely Cell Cycle Regulated and Is Required for Snf5 Binding

To determine the order by which Spt10, H3 K56 acetylation, and Snf5 function in regulating histone gene ex-

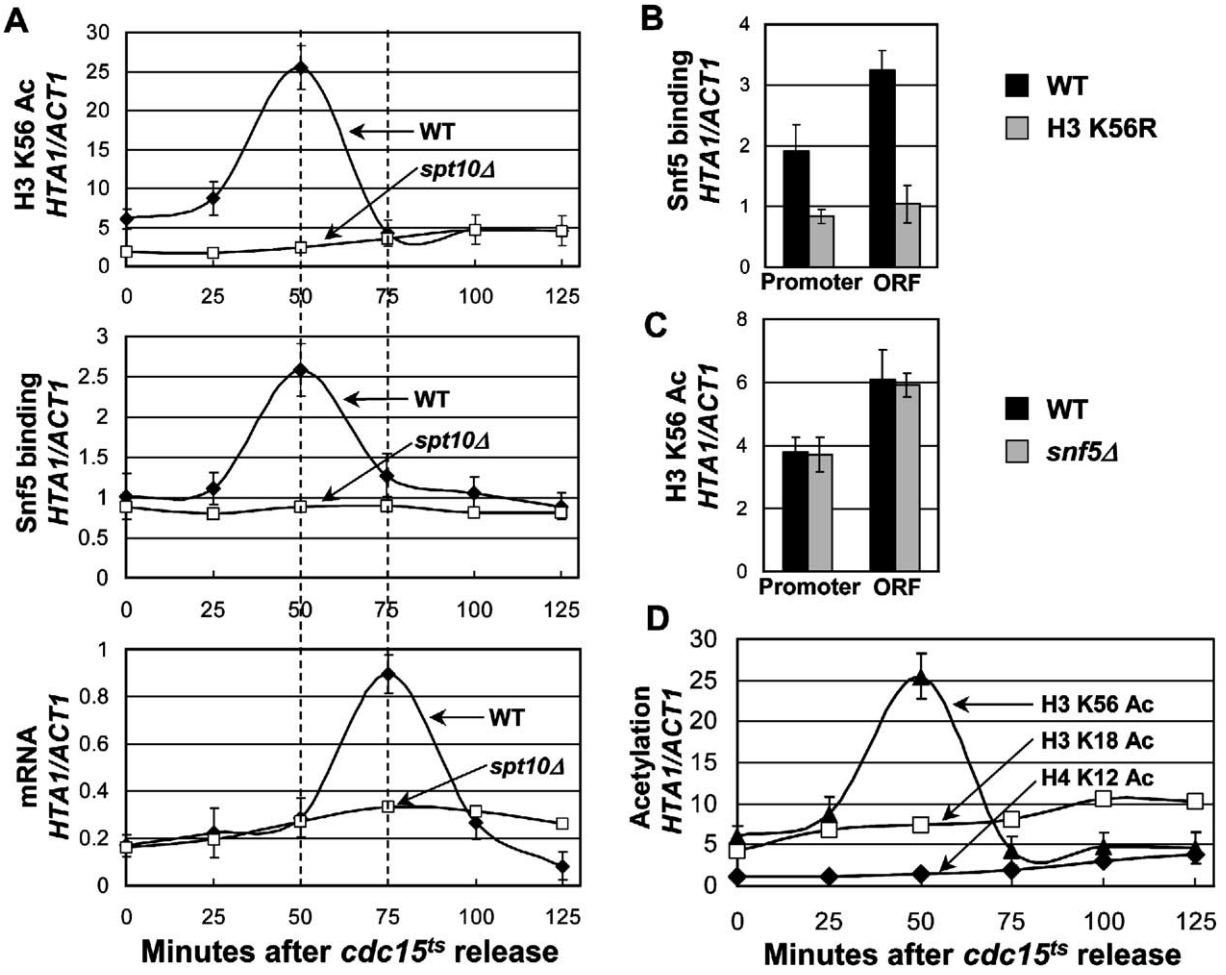

Figure 5. H3 K56 Acetylation Is Cell Cycle Regulated and Is Required for Snf5 Binding at the *HTA1* Gene

(A) Samples were taken at the indicated intervals after *cdc15*^{ts} cells were released from the restrictive temperature (37°C) to permissive temperature (23°C). H3 K56 acetylation and Snf5 binding peak simultaneously at about 50 min after release at the *HTA1* coding region, which precedes the mRNA expression peak at about 75 min after release. *spt10Δ* abolishes K56 acetylation, Snf5 binding, and mRNA expression peaks at the *HTA1* coding region.

(B) H3 K56R mutation disrupts Snf5 binding at both the promoter and coding region of the *HTA1* gene.

(C) *snf5Δ* does not affect H3 K56 acetylation at either the promoter or coding region of the *HTA1* gene.

(D) Only acetylation of H3 K56, but not H3 K18 nor H4 K12, is cell cycle regulated at the *HTA1* coding region. All of the ChIP and RT-PCR data are normalized to an internal control (*ACT1*). The results are averages of three independent experiments with error bars shown for standard deviations.

pression, we first examined when in the cell cycle these events occur. Histone *HTA1* gene expression is strictly cell cycle regulated (Spellman et al., 1998), and its expression peaks at about 75 min after shifting synchronized *cdc15*^{ts} cells from the restrictive temperature of 37°C to the permissive temperature of 23°C (see Experimental Procedures and Figure 5A). We find that H3 K56 acetylation is also cell cycle regulated and peaks 25 min earlier than the peak of histone *HTA1* gene expression at both the promoter (data not shown) and coding region (Figure 5A) of the *HTA1* gene. Interestingly, we find at the *HTA1* coding region that K56, but neither H3 K18 (affected by *SPT10*) nor H4 K12 (unaffected by *SPT10*), is acetylated in a cell cycle-specific manner (Figure 5D). Similar findings were made at the *HTA2* gene (Figures S5B and S5C). These data underscore the important role of K56 acetylation in gene regulation in S phase. In order to rule out the possibility that cycle-specific K56 acetylation is caused by heat shock of growing cells at the restrictive temperature of 37°C, we also examined the H3 K56 acetylation pattern at the *HTA2* gene coding region using cells synchronized by α factor arrest in G1 (Spellman et al., 1998). In cells that have been synchronized by α factor arrest at 30°C, H3 K56 acetylation peaks at 30 min after release from α factor, which is 10 min earlier than the expression peak (Figure S5A). Thus, K56 acetylation occurs in a cell cycle-specific manner significantly earlier than histone gene expression in S phase.

We wished to then determine when in the cell cycle K56 acetylation and Snf5 binding take place at *HTA1* relative to its gene expression. ChIP analysis demon-

strates that the peak of Snf5 binding is coincident with H3 K56 acetylation at both the *HTA1* promoter and coding region (Figure 5A). To ask whether Spt10 and K56 acetylation are required for Snf5 binding, we examined both in an *spt10Δ* strain. We found that the absence of *SPT10* abolishes the cell cycle-specific peaks of H3 K56 acetylation, Snf5 binding, and mRNA expression at *HTA1* (Figure 5A) and *HTA2* genes (Figure S5B). Moreover, the substitution K56R results in dramatically decreased Snf5 binding at both the promoter (2.3-fold) and coding region (3.1-fold) of the *HTA1* gene (Figure 5B). However, H3 K56 acetylation at the *HTA1* gene promoter and ORF does not change significantly in the *snf5Δ* strain (Figure 5C). These data demonstrate that H3 K56 acetylation in S phase mediated by Spt10 is required for the cell cycle-specific recruitment of the SWI/SNF complex to the *HTA1* and *HTA2* genes enabling histone gene transcription.

K56 Acetylation Also Controls SWI/SNF Recruitment at the *SUC2* Gene

SUC2 is a gene that is also regulated by the SWI/SNF remodeling complex (Geng and Laurent, 2004). Therefore, to examine a nonhistone gene, we asked whether K56 acetylation is important for Snf5 recruitment and *SUC2* activity. Using RT-PCR, we compared *SUC2* gene expression upon induction (switching the carbon source from glucose to raffinose) in wt and H3 K56R mutant strains. We found that K56R severely impairs the activation of the *SUC2* gene (10.8-fold increase of expression in wt as compared to 2.8-fold increase in K56R mutant strain after 90 min induction; Figure S6A). By ChIP, we also demonstrate that in wt cells, H3 K56 acetylation increases at both the promoter (2.1-fold) and ORF (4.5-fold) of the *SUC2* gene when *SUC2* is activated in raffinose (Figure S6B). These increases, especially at the promoter, are likely to be an underestimate of the actual increase in acetylation of K56, since gene activity is accompanied by considerable nucleosome loss at the promoter (Boeger et al., 2003; Reinke and Horz, 2003) for which we did not correct in these experiments. Finally, the H3 K56R mutation disrupts Snf5 binding (~2 fold) to the *SUC2* gene when *SUC2* is activated (Figure S6C). We conclude that *SUC2* is also regulated by acetylation of K56.

Whole-Genome Expression Analysis Shows Positive Correlations between the Expression Profiles of *spt10Δ*, K56R, and *snf5Δ* Mutants

To determine how Spt10, K56, and Snf5 affect gene expression genome-wide, we examined whole-genome expression profiles in *spt10Δ*, K56R (whose charge mimics unacetylated K56), and *snf5Δ* mutant strains. We found there to be a strong positive correlation between the expression profiles of *spt10Δ* and K56R mutant cells (R = 0.49; Figure S7B). *spt10Δ* showed a lower correlation (R = 0.21) with K56G, which replaces the lysine with an uncharged amino acid (Figure S7B). We also compared our K56G and K56R expression profiles to that of a *gcn5Δ* strain (Lee et al., 2000). The correlation values are R = 0.11 (*gcn5Δ*-K56R) and R = 0.08 (*gcn5Δ*-K56G), indicating that Gcn5 may not be involved in K56 acetylation. There are 108 and 150 genes downregulated >2-fold in *spt10Δ* and K56R mutants, respectively. Between these two gene sets, we found a highly significant overlap of 33 genes (p = 2.2E-28; Figure S7C). These data strongly suggest a functional connection between Spt10 and K56 acetylation in regards to genome-wide gene expression. We found a lesser but still positive correlation between the expression profiles of *snf5Δ* and K56R mutants (R = 0.19), suggesting that the K56R mutation affects the expression of a subset of genes that are Snf5 dependent. Thus, H3 K56 acetylation may reflect one of several pathways that contribute to SWI/SNF recruitment.

One of these pathways may involve cell cycle-specific expression. We compared our K56 acetylation microarray data to the whole-genome cell cycle-specific gene expression data (Spellman et al., 1998). Among the top 123 hyperacetylated ORFs (>1.6-fold), 98 genes have their cell cycle expression data available. Among those 98 genes, 32 were found to be cell cycle regulated with their expression peaks in diverse phases during the cell cycle (Table S1). The comparison shows that there is a statistically significant overlap between cell cycle-regulated genes and K56 hyperacetylated genes as determined by the hypergeometric distribution value (p = 1.8E-06; Figure S7A).

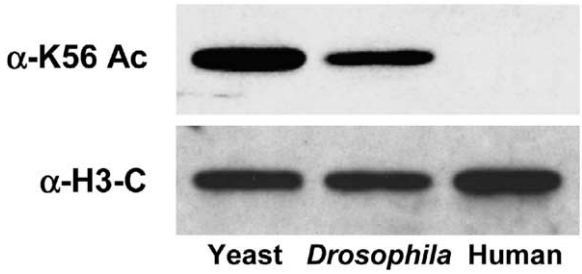

Figure 6. Conservation of H3 K56 Acetylation between Yeast and Flies

Whole-cell extracts prepared from *S. cerevisiae* (yeast), S2 cells of *D. melanogaster* (*Drosophila*), and HeLa cells (human) were resolved by 15% SDS-PAGE, transferred to nitrocellulose membrane, and probed with α-K56 Ac and α-H3-C as a loading control.

H3 K56 Acetylation Is Conserved between Yeast and *Drosophila*, but Not in Human Cells

Finally, we wished to know the extent to which K56 acetylation is conserved in evolution. Using the highly specific α-K56 Ac antibody (Figure S2), we examined the presence of H3 K56 acetylation among different organisms by Western blot. As shown in Figure 6, the α-K56 Ac antibody strongly immunoreacts with histones in the whole-cell extracts of yeast and S2 cells of *Drosophila melanogaster* but not that of HeLa cells. We also see no crossreaction of α-K56 Ac antibody to bulk histones of calf and chicken (data not shown). This is unlikely to be due to sequence differences in these organisms in the peptide epitope recognized by the antibody. While the peptide used (IRRFQKSTELLC) has a single amino acid substitution between yeast and mammals, this substitution (F→Y) is also found in *Drosophila*, yet fly histone H3 crossreacts strongly with the

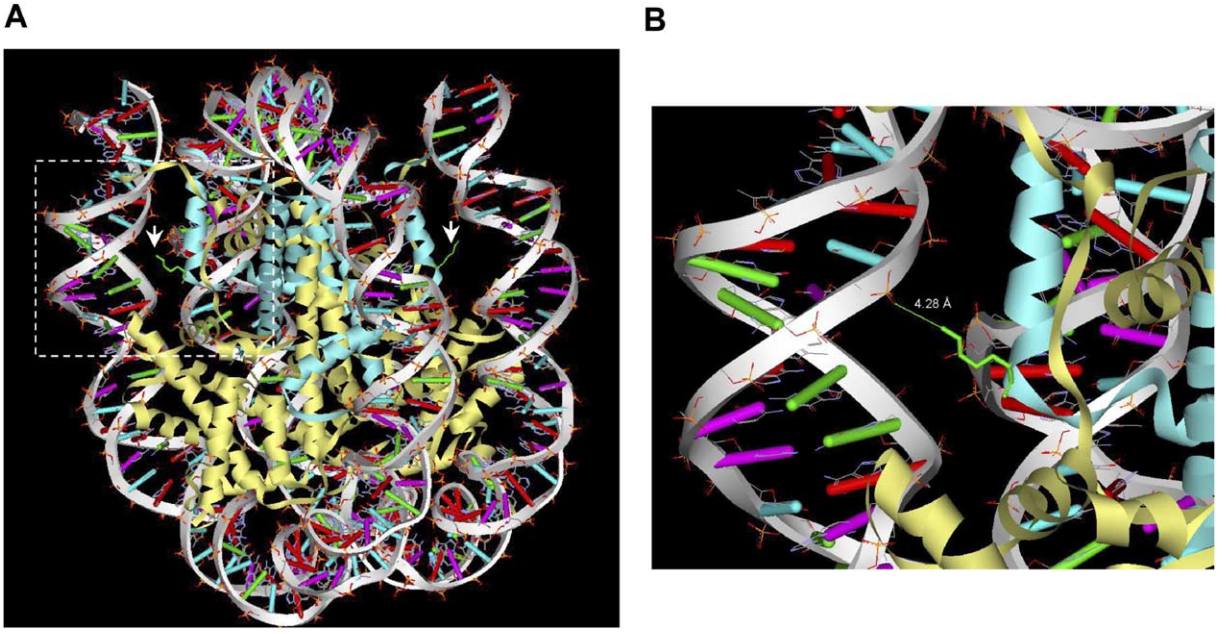

Figure 7. H3 K56 Is Located at the Entry-Exit Points of DNA Wrapped around the Histone Octamer

(A) The crystal structure of the yeast nucleosome core particle (Luger et al., 1997a; White et al., 2001) shows that two H3 lysine 56 residues are located at the entry and exit points of the DNA superhelix. Two histone H3 proteins are highlighted in blue and all other histones are colored in yellow. Two lysine 56 residues in H3 proteins are depicted in green and indicated by white arrows. The region within the white dashed line box is enlarged and shown in (B).

(B) Lysine 56 is located at the end of H3 αN helix and forms an electrovalent bond with the phosphate group of the DNA at a distance of 4.28 Å. Figures were generated using Webview according to the coordinates under accession number 1ID3 in the Protein Data Bank (White et al., 2001).

anti-yeast K56 Ac antibody. This result indicates the presence of H3 K56 acetylation in yeast and flies but not in mammals where K56 is likely to be methylated instead (Zhang et al., 2003).

Discussion

In this study, we have identified K56 of histone H3 by mass spectrometry as a novel acetylation site in *S. cerevisiae*. In order to investigate the genome-wide occurrence and biological function of this modification, we have generated an antiserum specific to H3 acetylated at K56 and have shown that hyperacetylation of K56 through the putative acetyltransferase Spt10 preferentially occurs at a subset of actively transcribed genes, such as those coding for histones. We also showed that K56 acetylation near the entry-exit points of the DNA superhelix as it wraps around the nucleosome is required for recruiting the nucleosome remodeling complex SWI/SNF and for subsequent histone gene activity.

Several lines of evidence suggest that Spt10 is a HAT that is responsible for H3 K56 acetylation in *S. cerevisiae*. First, Spt10 binds to all the histone genes and *spt10Δ* affects K56 acetylation at all histone genes (Figures 1 and 2). This is especially evident in synchronous cells in which *spt10Δ* completely abolishes the prominent peak of K56 acetylation preceding the mRNA expression peak in S phase (Figures 5A and S5B). Second, Spt10 shares four conserved regions spanning over 100 residues found in other HATs including Gcn5 (Neuwald and Landsman, 1997), and a HAT domain mutation (*spt10-199*) reduces K56 acetylation and histone gene expression in a manner similar to that of *spt10Δ* (Figures 3B and 4B). Third, the transcriptional defects of *spt10Δ* and K56R are similar whether at single genes (Figure 4) or genome-wide (Figure S7). There is a strong and specific correlation (R = 0.49) between the expression profiles of *spt10Δ* and K56R mutant cells (Figure S7B), and we see a highly significant overlap (p = 2.2E-28) between those genes downregulated in *spt10Δ* and K56R mutants (Figure S7C). While neither Hess et al. (2004) nor our laboratory (data not shown) were able to demonstrate in vitro HAT activity for Spt10, our data indicate that the Spt10 is likely to be a HAT that determines K56 acetylation. Interestingly, the effect of *spt10Δ* on K56 is strongest on cells in S phase. In asynchronous cells, there is considerable K56 acetylation remaining at certain histone genes in the *spt10Δ* mutant (Figure 1A). Moreover, *spt10Δ* has but a minor effect (<15% decrease) on H3 K56 acetylation of bulk histones examined by Western blot (data not shown). Therefore, while there is likely to be more than one HAT that acetylates K56, Spt10 is the major HAT that modifies K56 in an S phase-specific manner.

It was noted above that *SPT10* is required for acetylation not only of H3 K56 but also K18 and K9. Yet we find that K56 mutation strongly affects histone gene expression while K18 does not (Figure 4C). Interestingly,

we find at the *HTA1* and *HTA2* coding regions that only K56 is acetylated in a cell cycle-specific manner unlike H3 K18 and the control H4 K12 site that is unaffected by Spt10 (Figures 5D, S5B, and S5C). This is expected for H4 K12; however, it is surprising that acetylation of two sites both strongly affected by the same enzyme should be acetylated so differently during the cell cycle (Figure 5D). These data are consistent with our finding (above) that there is only a correlation R = 0.3 between acetylation of H3 K56 and H3 K18. Thus, K18 acetylation is likely occurring through a different pathway involving Spt10 and possibly other HATs, and it is the unique cell cycle-specific acetylation of K56 by Spt10 that regulates histone gene expression.

The discovery of histone modifications in the globular domains of calf histones (Zhang et al., 2003) has led to the proposal that nucleosome remodeling complexes use the energy of ATP hydrolysis to expose histone sites in the globular domain and thus allow their acetylation (Cosgrove et al., 2004). Our data argue instead that acetylation of the globular domain at the entry-exit points of the DNA superhelix as it wraps around the nucleosome leads to nucleosome remodeling by SWI/SNF. How K56 acetylation recruits SWI/SNF is unknown, and we have no evidence for its direct interaction with acetylated K56. Moreover, the whole-genome expression profiles of *snf5Δ* and K56R mutant cells are correlated with each other relatively weakly (R = 0.19; Table S1). Therefore, SWI/SNF is likely to be recruited to different genes through different pathways. K56 acetylation serves as one such pathway and in the case of the histone genes is required primarily during S phase.

K56 Acetylation Is Likely to Regulate Histone-DNA Interactions at the Entry-Exit Points of the DNA Superhelix Surrounding the Nucleosome

The crystal structure of the nucleosome (Luger et al., 1997a; White et al., 2001) shows that K56 is located at the end of an α-helical histone-fold extension of H3 (H3 αN). As shown in Figure 7A, H3 αN binds exclusively to the penultimate 10 base pairs of nucleosomal DNA at each entry and exit point of the superhelix (Luger et al., 1997a; White et al., 2001). Therefore, modulation of the interaction between H3 αN and nucleosomal DNA may serve as a gate at each entry-exit point to wrap and unwrap DNA from the nucleosome. The electrostatic interaction between the basic side chain of lysine 56 and phosphate group of the DNA at a distance of 4.28 Å should contribute to the binding of H3 αN to DNA (Figure 7B). Given that the size of an acetyl-group is ~3 Å, the acetylation of H3 K56 would likely disrupt the electrostatic interactions and histone DNA contacts of the H3 αN region. Given the importance of controlling histone DNA interactions at the entry-exit points in the unfolding of DNA from the nucleosome (Kassabov et al., 2003; Lorch et al., 2001), these data argue that Spt10 acetylates K56 to start DNA unwrapping (Li and Widom, 2004). This process may then be extended by SWI/SNF to cause more complete nucleosome remodeling. Interestingly, K56 is apparently monomethylated in calf (Zhang et al., 2003). Whether K56 methylation is a means of preventing acetylation of this site in order to allow an alternate means of protein recruitment and chromatin opening remains to be determined.

Experimental Procedures

Yeast Strains and Plasmids

Cell synchronization was performed using strains MMY001 (*bar1::HIS3*, for α factor arrest) and DLY350 (*cdc15^{ts}*, gift from Ted Weinert). *SPT10* was disrupted with a *TRP1* fragment in YDS2 (wt) and a kanMX-fragment in DLY350 (*cdc15^{ts}*) background (Longtine et al., 1998) to generate FXY20 (*spt10::TRP1*) and FXY21 (*spt10::KAN*), respectively. Plasmids pFX04 (H3 K56G) and pFX06 (H3 K56R) were constructed using the QuikChange Site-Directed Mutagenesis Kit (Stratagene) and confirmed by sequencing. H3 K56G (FXY17) and H3 K56R (FXY19) mutant strains were made for this work in RMY200 background as described (Mann and Grunstein, 1992). Other histone mutant strains used in this work are NSY268 (H4 K12R), NSY120 (H3 K14R), and NSY130 (H3 K18R) (Suka et al., 2001). The *snf5Δ* mutant and its background wt strain BY4741 were purchased from ATCC. Plasmids pRS315 (empty *LEU2* vector), pDH63 (*spt10-199 LEU2* 2 μm), pDH65 (*SPT10-WT LEU2* 2 μm), and FY2195 (Spt10-13xmyc) strain were kind gifts from Fred Winston. Those three plasmids were transformed into FXY21 to generate FXY22 (empty vector), FXY23 (*spt10-199*), and FXY24 (*SPT10-WT*) strains, respectively.

Yeast Media and Cell Synchronization

All yeast cultures were grown in YEPD medium unless otherwise noted. Experiments involving *SUC2* gene induction were carried out as described (Geng and Laurent, 2004), and 90 min induction time was used in this study. α factor arrest and release were performed essentially as described (Vogelauer et al., 2002). *cdc15*-based synchronization and release were done as described (Spellman et al., 1998). Strains FXY22, FXY23, and FXY24 were grown in synthetic complete medium lacking leucine to select for the plasmids.

Mass Spectrometry

Yeast core histones were purified from asynchronous culture as described (Edmondson et al., 1996) and separated by reverse-phase (RP) C4 HPLC (Zhang et al., 2004). The fraction corresponded to H3 was digested with trypsin or Arg_C (for quantification assays). The H3 digests were further separated by RP-HPLC and subjected to high-accuracy MALDI-TOF mass spectrometry analysis and nano-ESI/MS/MS sequencing (Zhang et al., 2002). Relative abundance of K56 acetylation was calculated by dividing the amount of acetylated peptide by the sum of acetylated and unacetylated peptides.

Peptide Synthesis, Antibody Generation, and Western Blot

All the H3 peptides used in this study (Figure S2A) were synthesized by the Biopolymer Synthesis Center at Caltech (Pasadena, California). A rabbit polyclonal antiserum was made as described (Suka et al., 2001) using a synthetic peptide containing yeast histone H3 residues 51–61(IRRFQKSTELLC) in which residue 56 was synthesized to contain acetyl-lysine. Specificity of this anti-H3 K56 acetylation (α-K56 Ac) antibody was further tested by ELISA, Western blot, and ChIP. For ELISA, K56 Ac peptide was conjugated to KLH as described by the manufacturer (Pierce) and coated to microtiter plates. The specific or unspecific H3 competitor peptides were tested in the competition assay for their ability to inhibit binding of α-K56 Ac to K56 Ac-KLH conjugate (Turner and Fellows, 1989). For Western blots, core histones were isolated from wt, H3 K56G, H3 K56R, and H3 K14R strains and immunoblotted with α-K56 Ac antibody at 1:2000. To compare H3 K56 acetylation in various species, core histones from yeast cells, chicken erythrocytes (Upstate), calf thymus (Sigma), and HeLa cells (Upstate) as well as recombinant *Xenopus* histone H3 (Upstate) were resolved by 15% SDS-PAGE, transferred to nitrocellulose membrane, and probed with α-K56 Ac at 1:2000. Whole-cell extracts were prepared from asynchronously growing *S. cerevisiae* cells and S2 cells of *D. melanogaster* and probed with α-K56 Ac at 1:2000 and α-H3-C as

described (Gunjan and Verreault, 2003). ChIP was performed as described below.

Chromatin Immunoprecipitation and DNA Microarrays

ChIP was performed essentially as described (Suka et al., 2001) on yeast cells grown to A600 of 1.0 in 50 ml liquid medium. For α-K56 Ac antibody, we used 2.5 μl per 50 μl lysate in ChIP. The highly specific antibodies against individual sites of acetylation in histone tails were used as described (Suka et al., 2001). We used the polyclonal anti-Snf5 antibody (Upstate) at 5 μl per 50 μl lysate in the Snf5 binding assay. For the Spt10-myc binding assay, the anti-Myc antibody (Upstate, 9E10) was used at 3 μl per 50 μl lysate. The antibody against histone H3 C terminus (3 μl per 50 μl lysate) was kindly provided by Dr. Alain Verreault. Primer sets amplifying different lengths of *ACT1* (310 bp and 150 bp) and *SPS2* (323 bp and 181 bp) fragments were used as internal controls in ChIP and RT-PCR to avoid overlapping other amplified bands. All primer sequences used in this study are available upon request. DNA microarray experiments were performed as previously described (Kurdistani et al., 2004; Robyr et al., 2002). The microarray containing IGRs were prepared as reported (Kurdistani et al., 2002), and those containing ORFs were purchased from University Health Networks, Toronto. To search for possible enrichment of the H3 K56 hyperacetylated genes in any of known categories of biological function, fitness, protein complexes, etc., we used the FunSpec website (Functional Specifications at http://funspec.med.utoronto.ca), which contains a comprehensive database of these features and performed statistical tests as described (Kurdistani et al., 2004). For expression microarrays, wt and mutant strains were grown in YEPD medium and collected at A_{600} of 0.5. Total RNA was isolated using Qiagen Rneasy Maxi Kit, and mRNA was further purified by using Qiagen Oligotex Maxi Kit. mRNA from the above preparation was reverse transcribed, labeled, and hybridized to the open reading frame microarrays. Correlation and hypergeometric distribution analyses were carried out using the corresponding function in Excel.

RT-PCR for mRNA Quantitation

Total RNA was prepared using hot-phenol extraction (Rundlett et al., 1998). We carried out a 25 μl RT reaction using 1× First-Strand Buffer (Invitrogen), 10 mM DTT, 0.75 mM dNTPs, 1 U μl^{-1} RNasin (Promega), 0.165 μg random 9-mer, 0.1 μg total RNA, and 8 U μl^{-1} M-MLV reverse transcriptase (Invitrogen) at 23°C for 10 min, 37°C for 60 min, and 70°C for 15 min. One microliter of this RT reaction was used in the subsequent quantitative PCR reaction.

Supplemental Data

Supplemental Data include seven figures and one table and can be found with this article online at http://www.cell.com/cgi/content/full/121/3/375/DC1/.

Acknowledgments

We are grateful to members of the Grunstein laboratory for critical comments and discussion throughout this work. We are especially grateful to Feng Qiao for help in preparing Figure 7, Alain Verreault for the histone H3 antibody, Fred Winston for the pRS315, pDH63, pDH65 plasmids and Spt10-13xmyc strain, and Ted Weinert for the *cdc15^{ts}* strain. This work was supported by Public Health Service National Institutes of Health grants GM23674 and GM42421 to M.G.

Received: November 24, 2004
Revised: February 28, 2005
Accepted: March 9, 2005
Published: May 5, 2005

References

Agalioti, T., Lomvardas, S., Parekh, B., Yie, J., Maniatis, T., and Thanos, D. (2000). Ordered recruitment of chromatin modifying and general transcription factors to the IFN-beta promoter. Cell *103*, 667–678.

Bannister, A.J., Zegerman, P., Partridge, J.F., Miska, E.A., Thomas, J.O., Allshire, R.C., and Kouzarides, T. (2001). Selective recognition of methylated lysine 9 on histone H3 by the HP1 chromo domain. Nature *410*, 120–124.

Bazett-Jones, D.P., Cote, J., Landel, C.C., Peterson, C.L., and Workman, J.L. (1999). The SWI/SNF complex creates loop domains in DNA and polynucleosome arrays and can disrupt DNA-histone contacts within these domains. Mol. Cell. Biol. *19*, 1470–1478.

Becker, P.B., and Horz, W. (2002). ATP-dependent nucleosome remodeling. Annu. Rev. Biochem. *71*, 247–273.

Boeger, H., Griesenbeck, J., Strattan, J.S., and Kornberg, R.D. (2003). Nucleosomes unfold completely at a transcriptionally active promoter. Mol. Cell *11*, 1587–1598.

Carmen, A.A., Milne, L., and Grunstein, M. (2002). Acetylation of the yeast histone H4 N terminus regulates its binding to heterochromatin protein SIR3. J. Biol. Chem. *277*, 4778–4781.

Cosgrove, M.S., Boeke, J.D., and Wolberger, C. (2004). Regulated nucleosome mobility and the histone code. Nat. Struct. Mol. Biol. *11*, 1037–1043.

Cosma, M.P., Tanaka, T., and Nasmyth, K. (1999). Ordered recruitment of transcription and chromatin remodeling factors to a cell cycle- and developmentally regulated promoter. Cell *97*, 299–311.

Dilworth, F.J., Fromental-Ramain, C., Yamamoto, K., and Chambon, P. (2000). ATP-driven chromatin remodeling activity and histone acetyltransferases act sequentially during transactivation by RAR/RXR In vitro. Mol. Cell *6*, 1049–1058.

Dimova, D., Nackerdien, Z., Furgeson, S., Eguchi, S., and Osley, M.A. (1999). A role for transcriptional repressors in targeting the yeast Swi/Snf complex. Mol. Cell *4*, 75–83.

Dorigo, B., Schalch, T., Bystricky, K., and Richmond, T.J. (2003). Chromatin fiber folding: requirement for the histone H4 N-terminal tail. J. Mol. Biol. *327*, 85–96.

Edmondson, D.G., Smith, M.M., and Roth, S.Y. (1996). Repression domain of the yeast global repressor Tup1 interacts directly with histones H3 and H4. Genes Dev. *10*, 1247–1259.

Geng, F., and Laurent, B.C. (2004). Roles of SWI/SNF and HATs throughout the dynamic transcription of a yeast glucose-repressible gene. EMBO J. *23*, 127–137.

Geng, F., Cao, Y., and Laurent, B.C. (2001). Essential roles of Snf5p in Snf-Swi chromatin remodeling in vivo. Mol. Cell. Biol. *21*, 4311–4320.

Gunjan, A., and Verreault, A. (2003). A Rad53 kinase-dependent surveillance mechanism that regulates histone protein levels in *S. cerevisiae*. Cell *115*, 537–549.

Hassan, A.H., Neely, K.E., and Workman, J.L. (2001). Histone acetyltransferase complexes stabilize swi/snf binding to promoter nucleosomes. Cell *104*, 817–827.

Hecht, A., Laroche, T., Strahl-Bolsinger, S., Gasser, S.M., and Grunstein, M. (1995). Histone H3 and H4 N-termini interact with SIR3 and SIR4 proteins: A molecular model for the formation of heterochromatin in yeast. Cell *80*, 583–592.

Hess, D., Liu, B., Roan, N.R., Sternglanz, R., and Winston, F. (2004). Spt10-dependent transcriptional activation in Saccharomyces cerevisiae requires both the Spt10 acetyltransferase domain and Spt21. Mol. Cell. Biol. *24*, 135–143.

Kassabov, S.R., Zhang, B., Persinger, J., and Bartholomew, B. (2003). SWI/SNF unwraps, slides, and rewraps the nucleosome. Mol. Cell *11*, 391–403.

Kingston, R.E., and Narlikar, G.J. (1999). ATP-dependent remodeling and acetylation as regulators of chromatin fluidity. Genes Dev. *13*, 2339–2352.

Krebs, J.E., Kuo, M.H., Allis, C.D., and Peterson, C.L. (1999). Cell cycle-regulated histone acetylation required for expression of the yeast HO gene. Genes Dev. *13*, 1412–1421.

Kurdistani, S.K., Robyr, D., Tavazoie, S., and Grunstein, M. (2002). Genome-wide binding map of the histone deacetylase Rpd3 in yeast. Nat. Genet. *31*, 248–254.

Kurdistani, S.K., Tavazoie, S., and Grunstein, M. (2004). Mapping global histone acetylation patterns to gene expression. Cell *117*, 721–733.

Lachner, M., O'Carroll, D., Rea, S., Mechtler, K., and Jenuwein, T. (2001). Methylation of histone H3 lysine 9 creates a binding site for HP1 proteins. Nature *410*, 116–120.

Ladurner, A.G., Inouye, C., Jain, R., and Tjian, R. (2003). Bromodomains mediate an acetyl-histone encoded antisilencing function at heterochromatin boundaries. Mol. Cell *11*, 365–376.

Langst, G., and Becker, P.B. (2001). ISWI induces nucleosome sliding on nicked DNA. Mol. Cell *8*, 1085–1092.

Lee, T.I., Causton, H.C., Holstege, F.C., Shen, W.C., Hannett, N., Jennings, E.G., Winston, F., Green, M.R., and Young, R.A. (2000). Redundant roles for the TFIID and SAGA complexes in global transcription. Nature *405*, 701–704.

Li, G., and Widom, J. (2004). Nucleosomes facilitate their own invasion. Nat. Struct. Mol. Biol. *11*, 763–769.

Lieb, J.D., Liu, X., Botstein, D., and Brown, P.O. (2001). Promoter-specific binding of Rap1 revealed by genome-wide maps of protein-DNA association. Nat. Genet. *28*, 327–334.

Longtine, M.S., McKenzie, A., 3rd, Demarini, D.J., Shah, N.G., Wach, A., Brachat, A., Philippsen, P., and Pringle, J.R. (1998). Additional modules for versatile and economical PCR-based gene deletion and modification in Saccharomyces cerevisiae. Yeast *14*, 953–961.

Lorch, Y., Zhang, M., and Kornberg, R.D. (2001). RSC unravels the nucleosome. Mol. Cell *7*, 89–95.

Luger, K., Mader, A.W., Richmond, R.K., Sargent, D.F., and Richmond, T.J. (1997a). Crystal structure of the nucleosome core particle at 2.8 Å resolution. Nature *389*, 251–260.

Luger, K., Rechsteiner, T.J., Flaus, A.J., Waye, M.M., and Richmond, T.J. (1997b). Characterization of nucleosome core particles containing histone proteins made in bacteria. J. Mol. Biol. *272*, 301–311.

Mann, R.K., and Grunstein, M. (1992). Histone H3 N-terminal mutations allow hyperactivation of the yeast GAL1 gene in vivo. EMBO J. *11*, 3297–3306.

Matangkasombut, O., and Buratowski, S. (2003). Different sensitivities of bromodomain factors 1 and 2 to histone H4 acetylation. Mol. Cell *11*, 353–363.

Meersseman, G., Pennings, S., and Bradbury, E.M. (1992). Mobile nucleosomes—a general behavior. EMBO J. *11*, 2951–2959.

Narlikar, G.J., Fan, H.Y., and Kingston, R.E. (2002). Cooperation between complexes that regulate chromatin structure and transcription. Cell *108*, 475–487.

Neuwald, A.F., and Landsman, D. (1997). GCN5-related histone N-acetyltransferases belong to a diverse superfamily that includes the yeast SPT10 protein. Trends Biochem. Sci. *22*, 154–155.

Peterson, C.L., and Workman, J.L. (2000). Promoter targeting and chromatin remodeling by the SWI/SNF complex. Curr. Opin. Genet. Dev. *10*, 187–192.

Reinke, H., and Horz, W. (2003). Histones are first hyperacetylated and then lose contact with the activated PHO5 promoter. Mol. Cell *11*, 1599–1607.

Ren, B., Robert, F., Wyrick, J.J., Aparicio, O., Jennings, E.G., Simon, I., Zeitlinger, J., Schreiber, J., Hannett, N., Kanin, E., et al. (2000). Genome-wide location and function of DNA binding proteins. Science *290*, 2306–2309.

Robyr, D., Suka, Y., Xenarios, I., Kurdistani, S.K., Wang, A., Suka, N., and Grunstein, M. (2002). Microarray deacetylation maps determine genome-wide functions for yeast histone deacetylases. Cell *109*, 437–446.

Rundlett, S.E., Carmen, A.A., Suka, N., Turner, B.M., and Grunstein, M. (1998). Transcriptional repression by UME6 involves deacetylation of lysine 5 of histone H4 by RPD3. Nature *392*, 831–835.

Spellman, P.T., Sherlock, G., Zhang, M.Q., Iyer, V.R., Anders, K., Eisen, M.B., Brown, P.O., Botstein, D., and Futcher, B. (1998). Comprehensive identification of cell cycle-regulated genes of the yeast Saccharomyces cerevisiae by microarray hybridization. Mol. Biol. Cell *9*, 3273–3297.

Suka, N., Suka, Y., Carmen, A.A., Wu, J., and Grunstein, M. (2001). Highly specific antibodies determine histone acetylation site usage in yeast heterochromatin and euchromatin. Mol. Cell *8*, 473–479.

Turner, B.M., and Fellows, G. (1989). Specific antibodies reveal ordered and cell-cycle-related use of histone-H4 acetylation sites in mammalian cells. Eur. J. Biochem. *179*, 131–139.

Vogelauer, M., Rubbi, L., Lucas, I., Brewer, B.J., and Grunstein, M. (2002). Histone acetylation regulates the time of replication origin firing. Mol. Cell *10*, 1223–1233.

White, C.L., Suto, R.K., and Luger, K. (2001). Structure of the yeast nucleosome core particle reveals fundamental changes in internucleosome interactions. EMBO J. *20*, 5207–5218.

Workman, J.L., and Kingston, R.E. (1998). Alteration of nucleosome structure as a mechanism of transcriptional regulation. Annu. Rev. Biochem. *67*, 545–579.

Zhang, K., Tang, H., Huang, L., Blankenship, J.W., Jones, P.R., Xiang, F., Yau, P.M., and Burlingame, A.L. (2002). Identification of acetylation and methylation sites of histone H3 from chicken erythrocytes by high-accuracy matrix-assisted laser desorption ionization-time-of-flight, matrix-assisted laser desorption ionization-postsource decay, and nanoelectrospray ionization tandem mass spectrometry. Anal. Biochem. *306*, 259–269.

Zhang, L., Eugeni, E.E., Parthun, M.R., and Freitas, M.A. (2003). Identification of novel histone post-translational modifications by peptide mass fingerprinting. Chromosoma *112*, 77–86.

Zhang, K., Siino, J.S., Jones, P.R., Yau, P.M., and Bradbury, E.M. (2004). A mass spectrometric "Western blot" to evaluate the correlations between histone methylation and histone acetylation. Proteomics *4*, 3765–3775.